

Estimating dry matter and fat content in blocks of Swiss cheese during production using on-line near infrared spectroscopy

Carl Emil Eskildsen¹ , Karen Wahlstrøm Sanden¹, Sileshi Gizachew Wubshet¹, Petter Veje Andersen¹, Jorun Øyaas² and Jens Petter Wold¹

Abstract

Modern dairy factories produce thousands of cheese blocks per day. Cheese quality is partly defined by the concentration of dry matter and fat. In this study, we evaluated three different near infrared spectroscopy instruments for on-line determination of fat and dry matter in cheese blocks of approx. size 35 × 28 × 12 cm: scanning reflection (908–1676 nm), scanning interaction (760–1040 nm), and imaging interaction measurements (760–1040 nm). The near infrared measurements were performed on fresh cheese blocks in a pilot plant at three different critical control points (CCP): (CCP1) before pressing, (CCP2) after pressing, and (CCP3) after salting. A total of 160 cheeses from 10 production batches were measured. Whereas near infrared measurements were obtained from the surface of the cheese blocks, the reference analysis was done on a cross-section of the cheese blocks. In general, good results were obtained regressing the reference values onto the near infrared measurements using partial least squares regression. For example, using near infrared scanning reflection at CCP2 yielded root mean squared errors of cross-validation on 0.44% and 0.64% for fat and dry matter, respectively. Hence, surface chemistry of cheese blocks were representative for the average chemistry of the blocks. Furthermore, this study finds that it is possible to predict fat and dry matter at CCP3 based on near infrared measurements obtained at CCP1 earlier in the process. This enables improved control of the cheese making process, as it is possible to detect deviations from target quality early in the production process.

Keywords

Process analytical technology, on-line, production, cheese, dry matter, fat

Received 21 November 2018; accepted 15 May 2019

Introduction

An ever-increasing scale in dairy manufacturing makes process optimization an economic necessity. Raw material analysis, process control, and end-product testing are crucial steps in any industrial food production, and near infrared (NIR) spectroscopy may be used as an analytical tool throughout all steps.¹ In cheese production, a milk-clotting enzyme (rennet) is added to milk to promote coagulation. The coagulum is cut and cheese grains are pressed to drain moisture and whey. After pressing, the cheese is salted and left for ripening. Fat and dry matter (DM) content are important quality parameters for cheese ripening as well as final cheese quality.² The amount of DM is also decisive for the profitability of the process, and it is therefore important to control the process towards the desired quality.

NIR spectroscopy is a well-established method for rapid determination of fat, protein, and moisture in

cheese,³ and NIR spectroscopy is widely used in the dairy industry.⁴ Wittrup and Nørgaard⁵ and Čurda and Kukačková⁶ estimated fat and DM content in intact cheese using an NIR reflectance module equipped with an optical fiber. Karoui et al.⁷ and Lucas et al.⁸ estimated fat and DM content in grated processed cheese using NIR measurements in reflectance mode. These studies^{5–8} obtained comparable results (a root mean squared error of prediction of approx. 0.52% and 0.58% for fat and DM content,

¹Nofima AS, Norwegian Institute for Food and Fisheries Research, Tromsø, Norway

²TINE SA Jæren, Nærbø, Norway

Corresponding author:

Carl Emil Eskildsen, NOFIMA AS, Osloveien 1, Ås 1443, Norway.
Email: carl.eskildsen@nofima.no

respectively). In these studies,^{5–8} measurements were done using off-line lab-based instrumentation. Furthermore, measurements were done on grated or relatively small pieces of cheese with very good correspondence between NIR and chemical sampling.

Industrial produced cheese has a typical unit size of $40 \times 30 \times 20$ cm weighing approx. 20 kg. Swiss cheese appears as a rather homogeneous material but during production, the crude chemical composition (i.e. moisture, fat, and salt content) can vary within the cheese.² For instance, after salting, there will be an outer layer with more salt and water compared to the interior part of the cheese. Potential heterogeneity of the cheeses pose a sampling challenge related to acquiring representative NIR measurements of intact cheese blocks. To address this, we used three NIR spectroscopic systems with different sampling modes: (1) scanning interaction measurements, (2) imaging interaction measurements, and (3) scanning reflection measurements. Interaction measures deeper into the cheese, whereas reflection measures mainly at the surface. The scanning measurements will only measure a limited region of the cheese, whereas imaging will measure the entire surface area.

A large-scale dairy production can produce thousands of kg of cheese every day. Adamopoulos et al.⁹ show how NIR reflection can estimate fat, protein, and moisture in an on-line setting and thereby facilitate real-time process control, at six different critical control points (CCP), throughout a feta cheese production. In this study, we also obtain NIR measurements, in an on-line setting, to estimate fat and DM content in intact blocks of fresh Swiss cheese (i.e. before ripening). We acquired NIR spectra on blocks of cheese at three CCP: (CCP1) before pressing, (CCP2) after pressing, and (CCP3) after salting. Furthermore, we investigate whether NIR measurements acquired early in the process can be used to estimate fat and DM content in the cheese later in the process. This will enable the detection of batches that may be out of specification at an early stage and allow necessary control actions in production to afford the required quality specifications.

Materials and methods

Cheese samples

A total number of 160 cheeses were included in this study. Cheeses were made in a dairy pilot plant (under industrial conditions) through nine different batches. Each batch consisted of 18 cheeses. However, batch seven consisted of 12 cheeses, as milk was lacking to produce 18 cheese in this batch. In addition, four cheeses from the commercial dairy production line were included (batch 10). Variation in DM and fat content was induced by varying initial fat content of the milk between batches. Furthermore, variation in DM content was additionally ensured by varying the cutting time of the coagulum. Hence, increasing the time for

cheese grains to release whey and moisture and thereby increasing the DM content.

Each cheese weighed from 12 kg to 14 kg and was approx. $35 \times 28 \times 12$ cm in size. However, size varied between cheeses and between CCP. At CCP1, cheeses were thicker and varied up to about 4 cm in thickness from one cheese to another. Furthermore, the same cheese could vary 3 cm in thickness from one end to the other. At CCP2 and CCP3, cheese sizes were more uniform and weighed from 10 kg to 11 kg.

The sampling design is shown in Figure 1. NIR spectroscopic measurements were obtained on all 160 cheeses at CCP1 and CCP2. Within each batch, 50% of the cheeses (a total of 80 samples) were withdrawn for reference analysis at CCP2, while the remaining 50% of the cheeses were salted. At CCP3, the remaining 80 cheeses were measured with NIR spectroscopy again and referenced for fat and DM content.

Near infrared measurements

Near infrared scanning reflection. A low cost, miniature, and handheld NIR system was used for reflection measurements (MicroNIR, VIAVI Solutions Inc., Eningen, Germany). The instrument has two integrated tungsten lamps and collects spectra in the 908–1676 nm region with readings at every 6.2 nm intervals. The dispersing element is a linear filter with a 128 pixel InGaAs array as detector. The instrument samples an approx. circular area of 1 cm in diameter. The system was used in a hand held fashion for flexibility with regard to varying cheese thickness. Each cheese was scanned along a central line of the cheese, and the instrument was held at about 0.5 cm distance from the cheese surface. Hence, each cheese was sampled in a longitudinal line with a width of approx. 1 cm. The average spectrum from each cheese was used for analysis.

Near infrared scanning interaction. This prototype NIR instrument consists of two halogen light sources of 50 W, illuminating the sample in two rectangular areas with a size of 5×20 mm. The distance between the two illuminated regions is 10 mm. The system collects the signal in a small area of 4×4 mm, in interaction mode, between the two illuminated rectangles. Hence, the collected light has traveled from the illuminated region to the point of signal collection in depths down to 1–2 cm, depending on the material.¹⁰ The system measures at 15 wavelengths in the region 760–1040 nm with a spectral bandwidth of 20 nm. Calibration of hardware was done by a white reference, a barium sulfate with curved base. It was held under the instrument allowing the light to pass from the field of illumination to the field of view. The system does about 70 measurements per second and is thoroughly described elsewhere.¹¹ During measurement, the cheeses were moved so a longitudinal line of approx. 3 cm width and 1–2 cm depth was sampled from each cheese. To obtain good interaction measurements,

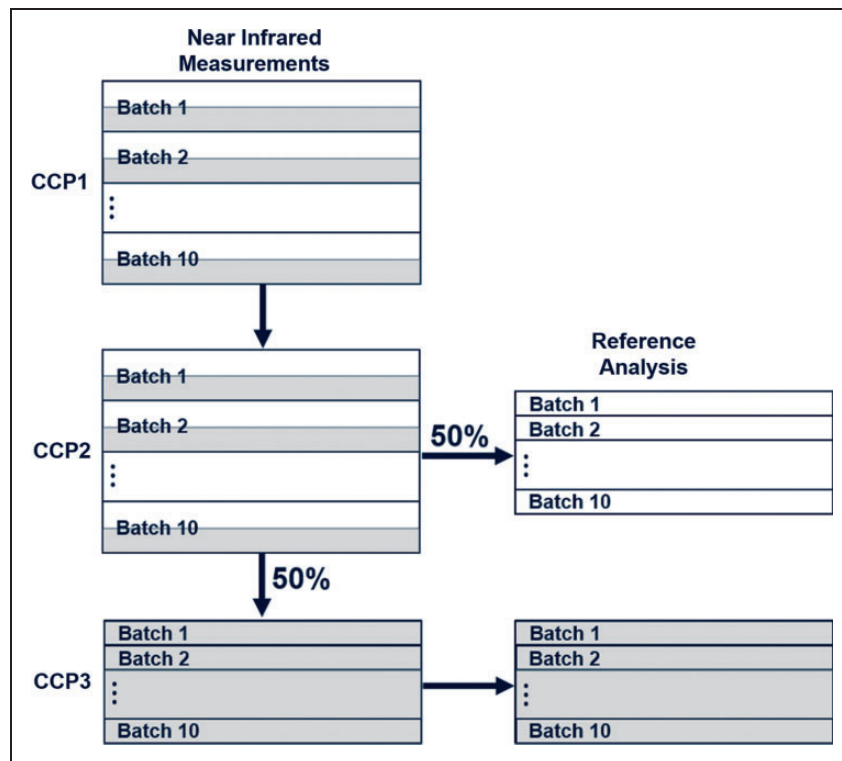


Figure 1. Sampling design showing critical control points (CCP). CCP1: non-pressed cheeses, CCP2: pressed cheeses, CCP3: pressed and salted cheeses.

it was important that the distance between cheese and instrument did not exceed about 1 cm. This was sometimes difficult to achieve, as the thickness within the single cheese varied. The average spectrum from each cheese was used for analysis.

Near infrared imaging interaction. QVision500 (TOMRA Sorting Solutions, Leuven, Belgium) was used for on-line hyperspectral NIR interaction imaging. The NIR instrument was equipped with a conveyor belt for the cheeses. The NIR instrument was based on interaction measurements where the light was transmitted into the cheese and then back scattered to the surface. Optical sampling depth in the cheese was approx. 10–15 mm but this was not documented. Each NIR scan took less than 3 s. The scanner was placed 30 cm above the conveyor belt without physical contact between samples and the instrument. The scanner collected hyperspectral images of 15 wavelengths between 760 and 1040 nm with a spectral resolution of 20 nm. The output per sample scan was an image of the conveyor belt with the cheese. Size of the image was 60 pixels in the direction perpendicular to belt movement and approx. 600 pixels in the direction of belt movement. Each pixel represented a spatial area of about 7×5 mm across and along the conveyor direction, respectively. The instrument is thoroughly described elsewhere.¹² In this study, the imaging capability was used for effective sampling, to obtain a representative average spectrum from each cheese. The average spectrum from each cheese was used for analysis.

Reference analysis

Fat and DM content were determined on-site at the dairy laboratory, following the standard procedures, using FoodScanTM (FOSS Analytical A/S, Hillerød, Denmark) and the commercial calibration model based on artificial neural network. The accuracy of the method on homogenized cheese (root mean squared error of prediction) was 0.30% and 0.35% for DM and fat, respectively. A cross-section (longitudinal side) of approx. 2 cm in thickness was cut from the center of each cheese. It was thoroughly homogenised into a finely grained powder with particle sizes in the range 1–2 mm and then used for reference analysis. We regarded this accurate at-line NIR laboratory method to be well suited as a reference for on-line NIR systems applied on big heterogeneous blocks of cheese.

Data analysis

Data were analyzed using MATLAB version R2016b (9.1.0.441655, MathWorks Inc., Natick, MA, USA). The NIR spectra were transformed from reflection/interaction (R) units into pseudo-absorbance units ($\log_{10}(1/R)$) and preprocessed by standard normal variate (SNV). Before calibration modeling, NIR spectra were additionally mean centered. The non-linear iterative partial least squares (PLS) algorithm was used for PLS regression.¹³ All PLS regression models were built with univariate and mean centered reference values (i.e. y-block) and validated using leave-one-out cross-

validation. The PLS regression models were evaluated by root-mean-square error of cross-validation (RMSECV).

Results and discussion

Table 1 shows descriptive statistics for DM and fat content. Both DM and fat content increase slightly from pressed cheeses (CCP2) to salted cheeses (CCP3) (Table 1). Fat content after pressing is highly correlated with fat content after salting (average values over batches). The same holds for DM content (data not shown). Fat and DM content correlate fairly well. Figure 2(a) shows the relationship between DM and fat content for pressed cheeses (CCP2) and Figure 2(b) shows the relationship for pressed and salted cheeses (CCP3). This is not surprising. First of all, cheeses (batches 1–9) are made in a pilot with intentionally varied settings. Moreover, fat contributes to the DM content.¹⁴ Furthermore, changes in cutting time and varying the amount of whey and moisture released from the gel affect both fat content and DM content. Figure 2 illustrates that there is a large variation in fat and DM content, also within batches.

Table 1. Descriptive statistics for dry matter (DM) and fat content.

Chemical component	Production step	Mean	SD
DM (%)	CCP2	55.5	1.6
	CCP3	56.8	1.5
Fat (%)	CCP2	24.8	3.0
	CCP3	25.2	3.0

CCP: critical control point; CCP2: pressed cheeses; CCP3: pressed and salted cheeses; SD: standard deviation.

Cross-validating PLS models over batches would be a natural choice here, but due to large within batch variation, it is decided to validate PLS models using leave-one-out cross-validation.

Figure 3 shows the SNV transformed NIR spectra obtained with the three instruments at CCP3. Spectra are colored according to DM content. Interaction measurements were obtained at shorter wavelengths than reflection measurements. Hence, prediction of fat content from the interaction measurements relates to the third overtone of C–H stretches and prediction of DM content additionally relates to the second overtone of N–H and O–H stretches. Prediction of fat content from the reflection measurements relates mainly to the second overtone of C–H stretches and the prediction of DM content additionally relates to the first overtone of N–H and O–H stretches.

Prior to regression modeling, two NIR interaction measurements on non-pressed cheese blocks from batch 4 were removed as outliers. These cheese blocks varied much in thickness. The longer the distance between the cheese and the interaction instrument, the higher share of the signal is surface reflectance, resulting in remarkably higher intensity throughout the entire spectrum, as compared with the other samples.

Figure 4 shows predictions of fat and DM content based on reflection measurements on pressed and salted cheeses (CCP3). Results from all regression models are summarized in Figure 5. The x-axis in Figure 5 specifies the production step used for calibration modeling. Hence, *X-block: CCP2* specifies that the NIR measurements were obtained at CCP2 (i.e. after pressing the cheeses). Similarly, *y-block: CCP2* specifies that the reference values were obtained at CCP2. Detailed results from all regression models are presented as a table in Appendix 1. The accuracy of the calibration models

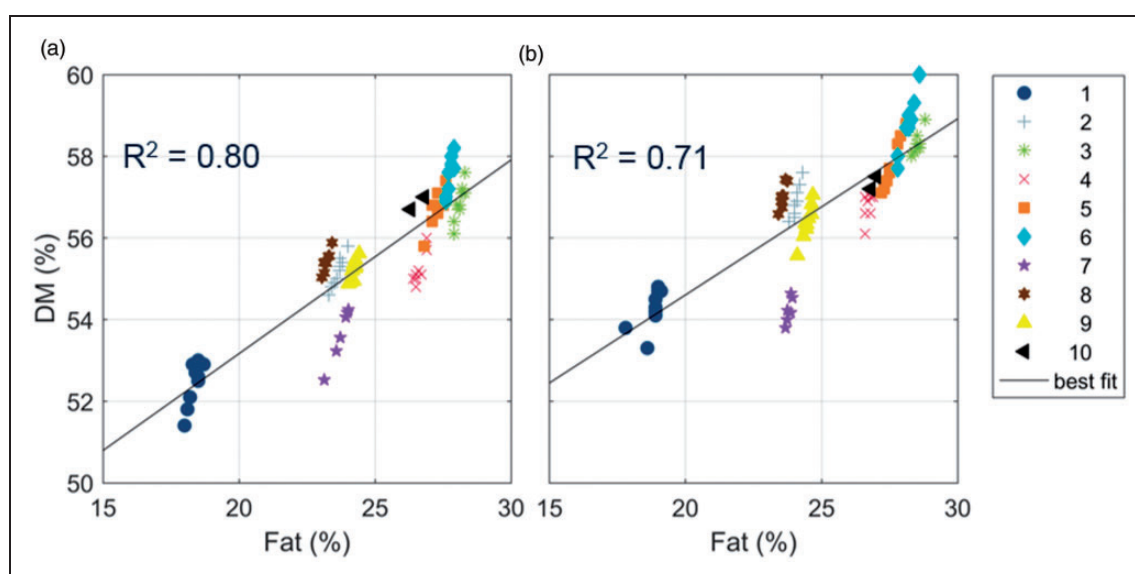


Figure 2. Reference values. (a) Critical control point 2, after pressing the cheeses. (b) Critical control point 3, after pressing and salting the cheeses. DM: dry matter. The legend indicates batches 1–10.

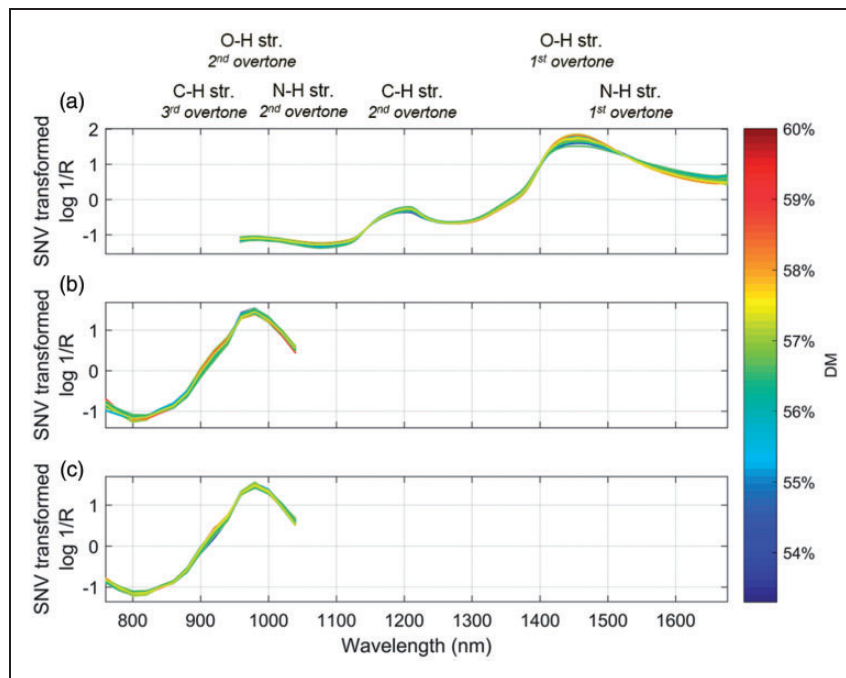


Figure 3. Standard normal variate (SNV) transformed near infrared spectra of pressed and salted cheeses. Spectra are colored according to dry matter (DM) content. (a) Scanning reflection. (b) Scanning interaction. (c) Imaging interaction.

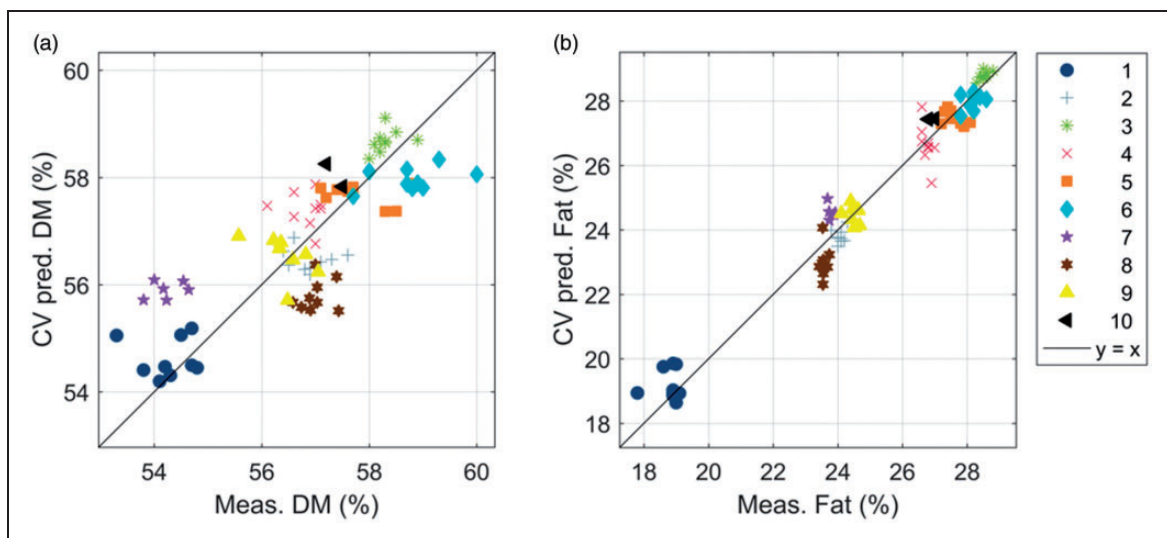


Figure 4. Measured versus cross-validated predicted values. Values were predicted by partial least squares regression applied to near infrared measurements from scanning reflection measurements. Near infrared measurements and reference values were obtained at critical control point 3, i.e. after pressing and salting the cheeses. (a) Prediction of dry matter (DM) content. (b) Prediction of fat content. The legend indicates batches 1-10.

obtained in this study vary, however, for the best models; the RMSECV values for both fat and DM content are comparable with previously reported results obtained with lab instruments.⁵⁻⁸ This suggests that it is possible to obtain NIR measurements on intact cheese block, which are representative for the average composition.

Figure 5 shows that the imaging system performs surprisingly worse than the scanning systems. We believe that these worse results relate to lower signal-to-noise

ratio for this system. The imaging interaction measurements are based on a flying beam, which measures in interaction mode while very rapidly scanning across the conveyor belt. The cheeses are compact with strong absorption, which results in rather noisy signals for this system. The scanning interaction system is equipped with high power light sources and optimized optics with the purpose of returning good signal-to-noise ratios of highly absorbing samples. The scanning reflection instrument measures mainly at the surface

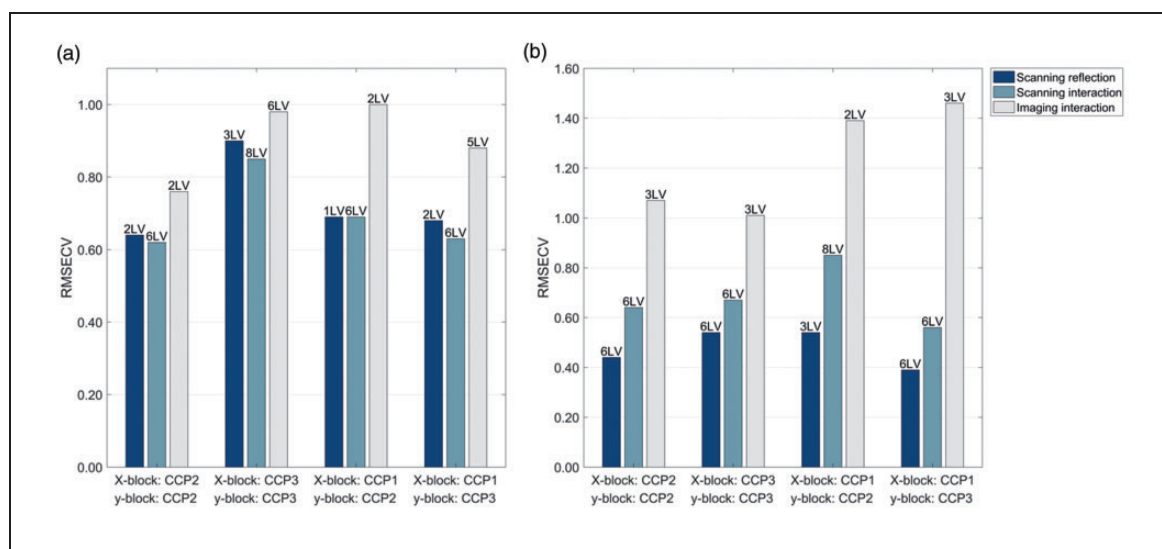


Figure 5. Results from partial least squares regression models. Root mean squared error of cross-validation (RMSECV) between measured and predicted values of: (a) dry matter content (%) and (b) fat (%). X- and y-blocks indicate input in the calibration models, where X-block is the spectral measurements and y-block is the reference values. CCP1: non-pressed cheeses, CCP2: pressed cheeses, CCP3: pressed and salted cheeses. The number of latent variables (LV) included in each model is stated above the bars.

and the light travels shorter distances in the cheese (as compared with the interaction measurements). Hence, more light is reflected to the instrument and a better signal-to-noise ratio is obtained.

Figure 5(a) shows that scanning interaction and reflection generally perform equally well when predicting DM content. However, PLS regression models based on scanning reflection measurements uses fewer latent variables (LVs). Furthermore, reflection measurements perform slightly better than interaction, when predicting fat content (Figure 5(b)). The reason for these differences is believed to relate to the wavelength ranges of the two instruments. The information in the interaction measurements are limited to higher overtones than that of the reflection measurements (Figure 3). Vibrational bands are more overlapping at higher overtones. This can clearly be seen in Figure 3(a) and (b), where three major bands important for prediction of DM and fat (i.e. third overtone of C–H and second overtone of O–H and N–H) are overlapping in a shorter wavelength range. Hence, the information on DM and fat content might be more easily available in the reflection measurements than in the interaction measurements. Moreover, as already mentioned above, the scanning interaction system is sensitive to variation in the distance between instrument and samples. Differences in this distance will introduce unwanted spectral variation between samples and result in more complex data. This could also be the reason for the higher number of LVs required to model the spectral data obtained with interaction measurements.

Figure 6 shows the regression coefficients obtained by PLS regression between NIR measurements and fat and DM content. Both NIR measurements and reference values were obtained at CCP3. Figure 6(a) shows

the regression coefficients acquired from the scanning reflection measurements. Due to lower complexity of the model predicting DM content (3 LV) compared to the model predicting fat content (6 LV), the regression vector for DM content is shorter. Nevertheless, the second overtone of C–H stretching vibration (round 1200 nm) seems dominating in both models. The regression vector for fat has surprisingly high coefficients around 1400 nm, which could relate to some C–H deformation. However, this is only a speculation. Figure 6(b) and (c) shows the regression coefficients acquired from the scanning interaction and the imaging interaction measurements, respectively. Both instruments work on the same spectral range and the regression coefficients for the two instruments look similar. Again, NIR measurements and reference values were obtained at CCP3. It is difficult to do proper interpretation of the regression vectors but the region just above 900 nm (third overtone of C–H stretching vibration) seems important in all models. Furthermore, the region round 800 nm seems important when predicting DM content. This region could relate to the third of N–H stretching vibration. Lastly, the regression vectors for DM have remarkably high coefficients just below 1000 nm. It could be that the regression vector from 950 nm to 1000 nm is orthogonal to the water signal and thereby cancels the information from water in the model. However, this is only a speculation.

The fact that models built on NIR reflection measurements predict fat and DM content well indicates that the cheeses were relatively homogeneous and that the salt gradient was similar from one sample to another. Slightly deeper NIR measurements with interaction did not provide better results.

We expected salt in the outer layer of the salted cheese to scatter near infrared light, reduce interaction

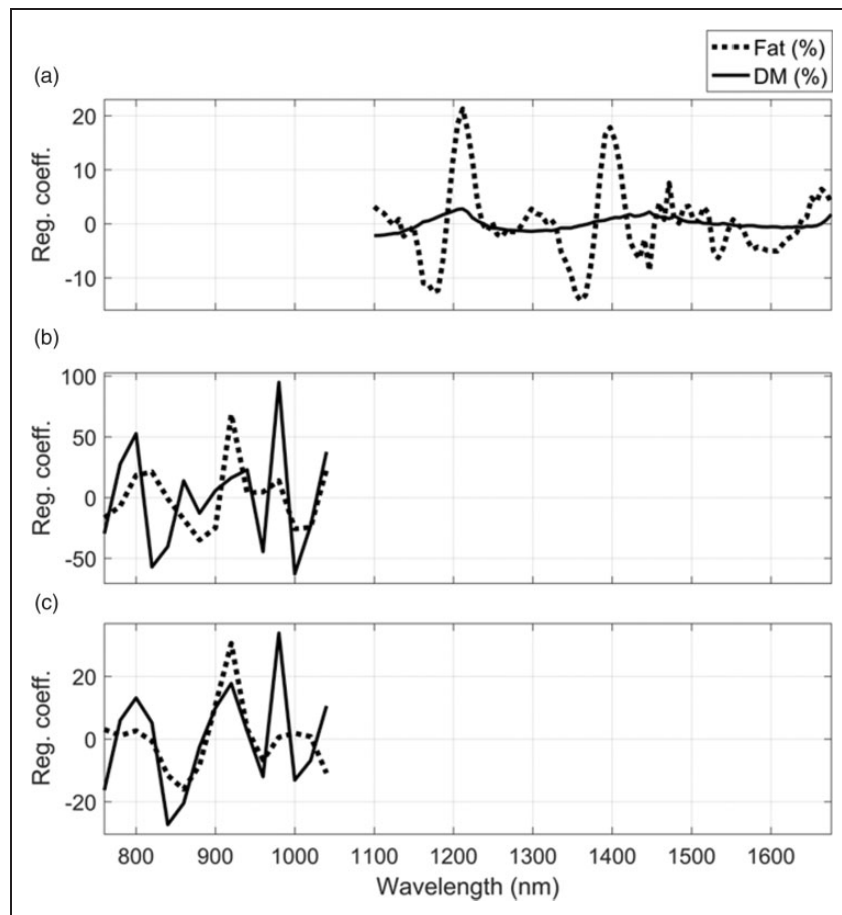


Figure 6. Regression coefficients estimated by partial least squares regression. Near infrared measurements and reference values obtained on pressed and salted cheeses. (a) Near infrared scanning reflection. (b) Near infrared scanning interaction. (c) Near infrared imaging interaction. Dotted lines: regression coefficient for estimating fat content. Solid lines: regressions coefficients for estimating dry matter (DM) content.

with the chemistry of the cheese and thereby provide worse PLS regression models. Hence, RMSECV values for models on pressed cheeses (CCP2) were expected to be lower than for models on pressed and salted cheeses (CCP3). This was the case for DM content (Figure 5(a)). However, this was not confirmed when predicting fat content (Figure 5(b)).

With regard to scanning reflection and interaction measurements, it is interesting to note that NIR measurements collected at CCP1 could be used to predict fat and DM content in cheeses at CCP2 and CCP3. The accuracy of these predictions was comparable with what we obtained with the NIR spectra collected at CCP2 and CCP3. The ability to predict DM and fat content at CCP2 and CCP3 based on spectra collected at CCP1 earlier in the process enables improved quality control, since action can be taken sooner. Such actions could be adjusting the pressing pressure to meet the desired DM content in the final products.

In the commercial process, DM will typically vary in the range from 55.5% to 60.0% (target is 58%) but can also be higher or lower if the batches are far from target due to unwanted process deviations. The span in DM and fat content used in this study is wide, but still relevant for both process optimization

and detection of batches that are outside specified quality limits.

Conclusions

This work illustrates that it is possible to obtain good estimates of fat and DM content in 12 kg cheese blocks based on on-line NIR scanning measurements. This means that the surface chemistry of the cheese blocks was representative of the average chemistry. Before using such an approach, one should be sure (e.g. by carefully sampling and examining the within cheese block variation) that this is actually the case for the relevant process. We also observed that it is possible to predict fat and DM content in pressed and salted cheeses based on NIR measurements on non-pressed cheese earlier in the process. This enables improved control of the cheese making process, as it could be possible to detect deviations from target quality early in the process.

Acknowledgements

The authors thank Bjørg Narum for assisting during data collection and TINE SA Jæren for providing materials, equipment, and man hours in their pilot plant and laboratory.

Declaration of conflicting interests

The author(s) declared no potential conflicts of interest with respect to the research, authorship, and/or publication of this article.

Funding

The author(s) disclosed receipt of the following financial support for the research, authorship, and/or publication of this article: The Norwegian Research Council through the project Innovative and Flexible Food Technology in Norway, iProcess, No. 255596 /E59, and the Norwegian Agricultural Food Research Foundation through the project FoodSMaCK – Spectroscopy, Modelling & Consumer Knowledge, No. 262308 /F40, funded the research presented here.

ORCID iD

Carl Emil Eskildsen  <https://orcid.org/0000-0003-3778-1771>

References

- Eskildsen CE, van den Berg F and Engelsen SB. Vibrational spectroscopy in food processing. In: Lindon J, Tranter GE and Koppenaal D (eds) *Encyclopedia of spectroscopy and spectrometry*, 3rd ed. Oxford: Academic Press, 2017, pp.582–589.
- Holroyd S. NIR analysis of cheese – a Fonterra perspective. *NIR news* 2011; 22: 9–11.
- Woodcock T, Fagan CC, O'Donnell CP, et al. Application of near and mid-infrared spectroscopy to determine cheese quality and authenticity. *Food Bioprocess Technol* 2008; 1: 117–129.
- Holroyd SE. The use of NIRS in the dairy industry: new trends and applications. *NIR news* 2017; 28: 22–25.
- Wittrup C and Nørgaard L. Rapid near infrared spectroscopic screening of chemical parameters in semi-hard cheese using chemometrics. *J Dairy Sci* 1998; 81: 1803–1809.
- Čurda L and Kukačková O. NIR Spectroscopy: a useful tool for rapid monitoring of processed cheeses manufacture. *J Food Eng* 2005; 61: 557–560.
- Karoui R, Mouazen AM, Dufour É, et al. A comparison and joint use of VIS-NIR and MIR spectroscopic methods for the determination of some chemical parameters in soft cheeses at external and central zones: a preliminary study. *Eur Food Res Technol* 2005; 223: 363–371.
- Lucas A, Andueza D, Rock E, et al. Prediction of dry matter, fat, pH, vitamins, minerals, carotenoids, total antioxidant capacity, and color in fresh and freeze-dried cheeses by visible-near-infrared reflectance spectroscopy. *J Agric Food Chem* 2008; 56: 6801–6808.
- Adamopoulos KG, Goula AM and Petropakis HJ. Quality control during processing of feta cheese – NIR application. *J Food Compos Anal* 2001; 14: 431–440.
- Wold JP. On-line and non-destructive measurement of core temperature in heat treated fish cakes by NIR hyperspectral imaging. *Innovative Food Sci Emerg Technol* 2017; 33: 431–437.
- O'Farell M, Wold JP, Høy M, et al. On-line fat content classification of inhomogeneous pork trimmings using multispectral near infrared interactance imaging. *J Near Infrared Spectrosc* 2010; 18: 135–146.
- Wold JP, Veiseth-Kent E, Høst V, et al. Rapid on-line detection and grading of wooden breast myopathy in chicken fillets by near-infrared spectroscopy. *PLoS One* 2017; 12: e0173384.
- Andersson M. A Comparison of nine PLS1 algorithms. *J Chemom* 2009; 23: 518–529.
- Verdier_Metz I, Coulon JB and Pradel P. Relationship between milk fat and protein contents and cheese yield. *Anim Res* 2001; 50: 265–371.

Appendix 1

Table 2. Results from partial least squares regression models.

Chemical component	Production step; NIR measurement	Production step; Reference measurement	Instrument	# LV	R ² CV	RMSECV (%)
DM (%)	CCP2	CCP2	Scanning reflection	2	0.83	0.64
			Scanning interaction	6	0.85	0.62
			Scanning imaging	2	0.78	0.76
	CCP3	CCP3	Scanning reflection	3	0.65	0.90
			Scanning interaction	8	0.68	0.85
			Scanning imaging	6	0.60	0.98
	CCP1	CCP2	Scanning reflection	1	0.82	0.66
			Scanning interaction	6	0.81	0.69
			Scanning imaging	2	0.61	0.99
	CCP1	CCP3	Scanning reflection	2	0.80	0.68
			Scanning interaction	6	0.83	0.63
			Scanning imaging	5	0.67	0.88

(continued)

Table 2. Continued

Chemical component	Production step; NIR measurement	Production step; Reference measurement	Instrument	# LV	R ² CV	RMSECV (%)
Fat (%)	CCP2	CCP2	Scanning reflection	6	0.98	0.44
			Scanning interaction	6	0.95	0.64
			Scanning imaging	3	0.87	1.07
	CCP3	CCP3	Scanning reflection	6	0.97	0.54
			Scanning interaction	6	0.95	0.67
			Scanning imaging	3	0.88	1.012
	CCP1	CCP2	Scanning reflection	3	0.97	0.54
			Scanning interaction	8	0.92	0.85
			Scanning imaging	2	0.76	1.39
	CCP1	CCP3	Scanning reflection	6	0.98	0.39
			Scanning interaction	6	0.96	0.56
			Scanning imaging	3	0.74	1.46

DM: dry matter; CCP: critical control point; CCP1: non-pressed cheeses; CCP2: pressed cheeses; CCP3: pressed and salted cheeses; # LV: number of latent variables included in the model; R²CV: coefficient of determination from cross-validation; RMSECV: root-mean-square error from cross-validation.